IEEE Access
Multidisciplinary ⋮ Rapid Review ⋮ Open Access Journal

Received December 13, 2020, accepted January 27, 2021, date of publication February 9, 2021, date of current version April 5, 2021.

Digital Object Identifier 10.1109/ACCESS.2021.3058288

Local Collision Avoidance Algorithm for a Unmanned Surface Vehicle Based on Steering Maneuver Considering COLREGs

DONG WANG[1,2], JIE ZHANG[1,2], JIUCAI JIN[2], AND XINGPENG MAO[1], (Member, IEEE)
[1]School of Electronics and Information Engineering, Harbin Institute of Technology, Harbin 150006, China
[2]First Institute of Oceanography, Ministry of Natural Resources, Qingdao 266061, China

Corresponding authors: Jie Zhang (zhangjie@fio.org.cn) and Jiucai Jin (jinjiucai@fio.org.cn)

This work was supported by the National Key Research and Development Program of China under Grant 2017YFC14052**.

ABSTRACT In order to sail safely in a marine environment with neighboring obstacles, a local collision avoidance algorithm based on a steering maneuver considering International Regulations for Preventing Collisions at Sea (COLREGs) is proposed for unmanned surface vehicles (USVs). In this paper, the algorithm consists of three parts: collision risk assessment, steering occasion determination, and navigation waypoint update. The collision risk assessment is used to judge a collision risk based on an analytical feasible angle interval by the closest point of approach method. The steering occasion determination provides a safe distance interval from an obstacle by analyzing a marginal steering angular velocity. The navigation waypoint update generates a temporary waypoint to navigate the USV and considers the overtaking, head-on, and crossing rules of COLREGs. The temporary waypoint is calculated based on a real-time optimal orientation angle, which is determined by an optimization objective function for angle deviation. The three parts for local collision avoidance are determined by a finite state machine. In simulations, a USV with actual dynamic constraints runs successfully in a static and dynamic multiobstacle environment, and the results indicate the feasibility and validity of the proposed algorithm.

INDEX TERMS Unmanned surface vehicle, collision avoidance, international regulations for preventing collisions at sea, finite state machine.

I. INTRODUCTION

Research on unmanned surface vehicles (USVs) has received increasing attention because of the rapidly increasing requirements of marine applications in recent years [1]. A robust and reliable guidance, navigation, and control (GNC) system is essential for a USV to undertake complex missions [1]–[3]. One important function of a GNC system is to plan a quasioptimal path while avoiding obstacles safely. Path planning usually includes global and local path planning. The former is based on known map information and is usually performed before the navigation of USVs. The latter is mainly used to avoid obstacles that are unknown prior and can be detected by onboard sensors within a local area.

Researchers have proposed many methods for the local collision avoidance of USVs. There are several types of local collision avoidance algorithms, such as the trajectory-based algorithm, behavior-based algorithm, and artificial intelligence algorithm.

In trajectory-based algorithms, appropriate trajectories or waypoints are generated for USVs. Svec *et al*. [4] utilized a fast heuristic search algorithm to find a trajectory in a space of candidate trajectories. The candidate trajectories are generated using a discretized set of dynamically feasible control actions and their corresponding nondeterministic state transitions. Soltan *et al*. [5] proposed a method that combines trajectory planning with real-time tracking control based on a sliding mode control law. The trajectory is defined by ordinary differential equations (ODEs), whose solution is the limit cycle. Du *et al*. [6] used a hydrodynamic model of the USVs to generate a trajectory unit that contains different orbit segments, and then the trajectory unit is searched on a grid map based on waypoint and heading choice rules. However, the shapes of trajectories in the trajectory unit are limited.

The associate editor coordinating the review of this manuscript and approving it for publication was Huiping Li.

Wang *et al*. [7] constructed a local normal distribution-based trajectory (LNDT) to avoid an obstacle. A set of waypoints with timestamps is extracted from the LNDT for the USV to complete obstacle avoidance by changing its speed and course. One disadvantage is that the adaptability of the trajectory needs to be improved.

In behavior-based algorithms, guidance velocities are generated and realized by the navigation controllers of USVs in real time to avoid collisions. The velocity obstacle (VO) method is a practical approach for determining valid velocities to avoid possible collisions. Fiorini and Shiller [8] introduced the basic theory of the VO method for robot motion planning in a dynamic environment. The universality of this method makes it also suitable for collision avoidance of USVs [9]. Nonlinear VO and probabilistic VO algorithms were introduced in [10] for collision avoidance with target ships whose trajectories are nonlinear and predictable, and a generalized VO algorithm was used to design a collision avoidance system by Huang *et al*. [11]. Line-of-sight (LOS) guidance and a VO algorithm were modified and applied in [12], and the performance and practical validity of the algorithm were demonstrated by real sea experiments. The VO can be treated as a set of constraints in the velocity space of the USV in order to avoid moving obstacles, and the USV selects a suitable velocity to avoid a collision [9]. Zhang *et al*. [13] and Tang *et al*. [14] proposed a local reflection collision avoidance algorithm for high-speed USVs in which the direction is altered by a directional steady-state model and the speed is altered by a translational velocity model. However, this algorithm is only suitable for static obstacle environments.

For artificial intelligence algorithms, two neuroevolutionary methods were used to build a collision avoidance system of USVs in [15]. Deep reinforcement learning algorithms [16], [17] have also recently been proposed for USV collision avoidance. These algorithms can achieve good collision avoidance effects in some situations. However, the main shortcoming is that the algorithm performance depends significantly on the training data.

The main dynamic obstacles on the ocean are ships, and their operations are required to obey the International Regulations for Preventing Collisions at Sea (COLREGs) [18]. Although COLREGs are regulations formulated for manned vessels, some rules can also be applied to USVs, and many studies have considered COLREGs for the collision avoidance of USVs. Benjamin *et al*. [19] proposed a behavior-based control framework that considers COLREGs with multiobjective optimization and interval programming. Kuwata *et al*. [9] combined the VO method with COLREGs by considering the three primary situations to navigate USVs safely in dynamic and cluttered environments. COLREGs were also taken into account in the replanning procedure for a rapid dynamic path planning system developed in [20]. Although a collision avoidance algorithm considering COLREGs may not be optimal in performance, it can effectively reduce collision risks when both the USV and the encounter vessel comply with COLREGs. Therefore, COLREGs should be considered in collision avoidance algorithms for USVs.

Most navigation and collision avoidance processes of USVs can be treated as the execution of a sequence of actions. When the actions can be divided into finite categories, a finite state machine (FSM) can be used to organize the process effectively. It is a useful computational model for both hardware and certain types of software [21]. In terms of ocean platform applications, a new programming architecture based on an FSM was presented by Woithe and Kremer [22]. In this FSM-based architecture, the programming model expresses autonomous underwater vehicle (AUV) missions at a higher level of abstraction, while the low-level software and hardware details are left to the compiler and runtime system. In order to improve the adaptability of AUVs in unknown obstacle environments, Xu and Feng [23] designed five basic obstacle avoidance behaviors and used an FSM to select a suitable avoidance behavior. Saad *et al*. [24] applied an FSM to execute a high-level hybrid strategy to coordinate a group of AUVs. For USV applications, Redding *et al*. [25] presented a collaborative mission planning, autonomy, and control technology (CoMPACT) using an FSM structure to enhance USV capabilities, where the FSM decision rules enable event-based or information-based transitions to govern behaviors of USVs. In the Autonomous Maritime Navigation (AMN) project, which was led by Spatial Integrated Systems, Inc. (SIS) with government support and direction from the Naval Surface Warfare Center (NSWC) Combatant Craft Division (NSWCCD), the mission-level behavior code is written as an FSM [26]. These successful applications imply the potential of FSM in the software architecture design for the collision avoidance process of USVs.

Although many novel algorithms for local collision avoidance in a cluttered environment have been proposed, local obstacle avoidance still limits the wide application of USVs. For example, the trajectories designed in trajectory-based algorithms usually have constraints on the number and shape. In addition, these trajectories are closely related to the control performance of USVs, and they may not be well realized by USVs in actual applications. The quantity and quality of training data seriously affect the performance of artificial intelligence algorithms. There may be situations that are not well-trained, in which the algorithms may perform unpredictable operations and may lead to serious consequences. The concept of behavior-based algorithms is in line with human habits in practical applications of ship operations. Most algorithms alter the velocity, including the speed and course of a USV in real time. However, accurate velocity may be difficult to achieve in an actual marine environment when it alters its speed and course simultaneously. In encounter situations, it is usually more difficult for the other encounter vessels to accurately determine the motion of the USV. As introduced in Rule 8 of COLREGs, alteration of course alone for USVs may be the most effective action in a maritime environment when it is made in good time and

is substantial [18]. In addition, when the USV runs at an economical speed, this is beneficial to the energy consumption in long-range applications. Therefore, we intend to develop an algorithm for USV local collision avoidance by altering USV headings alone under some dynamic constraints. COLREGs are also taken into account to reduce collision risks, and an FSM is designed to better organize the collision avoidance process of USVs.

In this paper, the proposed algorithm consists of three main parts that will be performed based on the specific collision situation: collision risk assessment, steering occasion determination, and navigation waypoint (NWP) update. In the collision risk assessment, the feasible angle interval considering COLREGs is calculated based on the concept of the VO method, and the risk of a collision is assessed by the closest point of approach (CPA) method. Based on the collision result, the steering occasion determination will be performed, and a safe distance interval is determined. If it is not satisfied, then the state of the USV will remain; otherwise, the NWP will be updated and is used to navigate the USV. The navigation and avoidance procedure based on the algorithm is reflected in the designed FSM.

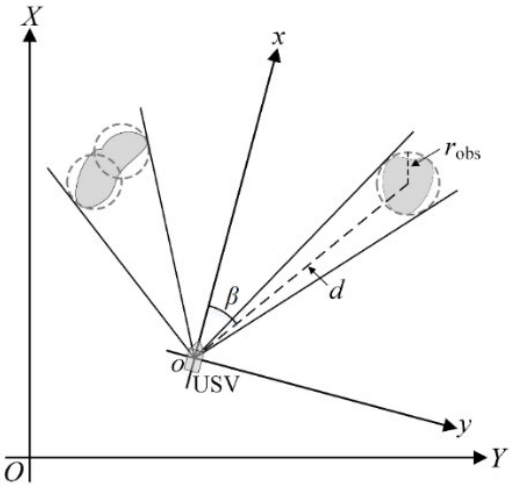

FIGURE 1. Schematic diagram of three coordinate systems and equivalent obstacles. Relative coordinate system *oxy* is dynamic with USV navigation. Obstacle is equivalent to circular obstacle with radius of r_{obs}, or multiple connected or overlapped circular obstacles when it is narrow and long. β is relative bearing angle of obstacle in *oxy*, and d is relative distance between obstacle and the USV.

II. ENVIRONMENT AND RISK ASSESSMENT MODELS

A. ENVIRONMENT MODEL

Three coordinate systems are established for the environment model, including an absolute coordinate system OXY, relative coordinate system oxy, and a polar coordinate system ox. As shown in Fig. 1, OXY is a rectangular coordinate system in geodesy. Its origin is determined when an application starts. The north and east are the positive directions of the X-axis and Y-axis. oxy is dynamic with the motion of the USV. Its origin is the USV center $\hat{C}$, and its x-axis and y-axis directions are the USV heading and the USV starboard direction. ox is the polar form of oxy. Angles in all coordinate systems begin from their own positive X-axis/x-axis and increase along a clockwise rotation.

It is assumed that the velocities of obstacles are nearly constant in a short time, and the basic information of these obstacles can be estimated, such as positions and sizes. Then, every obstacle can be equivalent to a circular obstacle with a radius of r_{obs}. Using the known USV position and heading, the relative bearing angle β in oxy and the relative distance d can be easily calculated. Furthermore, a narrow and long obstacle can be further equivalent to multiple connected or overlapped circular obstacles, as shown in Fig. 1.

B. RISK ASSESSMENT MODEL

A risk assessment model combining the CPA method and a simple risk level model is proposed to judge whether there will be a possible collision between a USV and obstacles.

In risk assessment applications of the CPA method, the distance to the closest point of approach (DCPA) and the time to the closest point of approach (TCPA) are usually used in combination. However, they have different priorities in risk assessment. DCPA can be used to judge the possibility of a collision first, and TCPA can be completely ignored when the judgment is no possible collision. Therefore, the risk assessment in this study is mainly dependent on DCPA, and the function of TCPA is reflected by the steering occasion (see part C of Section III).

TABLE 1. Defined Perimeters for risk assessment model.

Perimeter	Radius	Perimeter interpretation
B_O	r_O	Obstacle perimeter
B_P	r_P	Prohibition perimeter
B_W	r_W	Warning perimeter
B_B	r_B	Buffer perimeter

For the risk level model, four perimeters B_x with different radii r_x are defined as shown in Table 1, where the subscript x represents obstacle, prohibition, warning, or buffer, respectively. The surrounding area of an obstacle is divided into five regions S_y by the four perimeters, where the subscript y represents obstacle, prohibition, warning, buffer, or safety, respectively (see Fig. 2). S_O is the region with radius $r_O = r_{obs} + L_U/2$, where L_U is the USV length. The S_P is set for the detection deviations of obstacles. S_W is set considering the braking effect and lag in the USV control. S_B is a buffer region, and S_S is the safe region for a USV. When a USV sails into the S_B, $r_W < d_{CPA} \leq r_B$. In such situations, there is a small probability of collision, and collision avoidance maneuvers should be performed. When $d_{CPA} \leq r_W$, it is dangerous, and collision avoidance maneuvers must be performed. r_P, r_W, and r_B are determined based on the characteristics of the USV and the experience of operations.

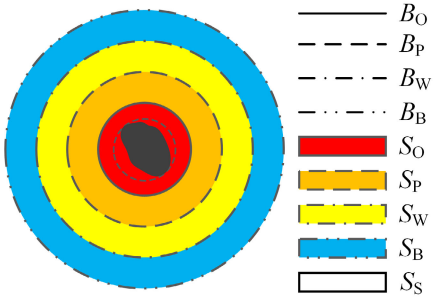

FIGURE 2. Risk level model. Black part is an obstacle. Surrounding area of obstacle is divided into five regions: S_Y (obstacle region S_O, prohibition region S_P, warning region S_W, buffer region S_B, and safety region S_S) by four perimeters B_X which are shown in Table 1. USV should perform maneuvers when it will sail into S_B, and maneuvers must be performed when USV will sail into S_W, S_P or S_O.

III. LOCAL COLLISION AVOIDANCE ALGORITHM

In the local collision avoidance algorithm considering COLREGs, a final navigation waypoint (NWP) result is set for the navigation of the USV. To determine the NWP in a collision risk situation, a risk assessment, steering occasion determination, and NWP update processes are selectively executed according to the detailed situation. For the risk assessment, a feasible angle interval $\boldsymbol{\Psi}$ is determined based on the similar concept of the VO method first, and then the collision risk is assessed based on the result of $\boldsymbol{\Psi}$ by using the risk assessment model. If there is no possible collision risk, then the NWP remains unchanged. Otherwise, a steering occasion considering COLREGs is determined to judge whether an action will be taken. When the steering occasion is satisfied, the NWP is updated by a navigation waypoint model; otherwise, the NWP remains unchanged again. Based on the above process, the feasible angle interval, COLREG selection, steering occasion, and navigation waypoint model used in the algorithm should be determined.

A. FEASIBLE ANGLE INTERVAL

The feasible angle interval $\boldsymbol{\Psi}$ represents a set of navigable USV headings with respect to a perimeter B_x. A $\boldsymbol{\Psi}$ was acquired in [27] under the condition that the detected obstacle is in front of a USV. As an extension, the more common result without this condition is introduced as follows.

TABLE 2. Velocities of USV and obstacle and relative velocity of obstacle with respect to USV.

Velocity	Description
(v_U,θ_U)	v_U and θ_U are speed and direction of USV. There is always $\theta_U = 0$.
(v_O,θ_O)	v_O and θ_O are speed and direction of obstacle.
(v_{UO},θ_{UO})	v_{UO} and θ_{UO} are relative speed and direction of obstacle with respect to USV.

1) CATEGORIES OF ANGLE INTERVALS

The velocity variables in oxy are listed in Table 2. The corresponding velocities in ox are represented by $\boldsymbol{V}_U = v_U e^{i\theta_U}$, $\boldsymbol{V}_O = v_O e^{i\theta_O}$, and $\boldsymbol{V}_{UO} = v_{UO} e^{i\theta_{UO}}$, which satisfy $\boldsymbol{V}_{UO} = \boldsymbol{V}_U - \boldsymbol{V}_O$ (see Fig. 3). The corresponding directions in OXY and oxy can be converted to each other through the USV heading ψ. When an angle is out of $\boldsymbol{U} = (-\pi, \pi]$, it can be mapped into $\boldsymbol{U}$ by plus or minus multiples of 2π. This mapping operation is defined as the function $f_M(\theta)$. For an actual USV, v_U and ψ can be acquired by the navigation system, while (v_O, θ_O), and (v_{UO}, θ_{UO}) can be estimated by the obstacle detection system.

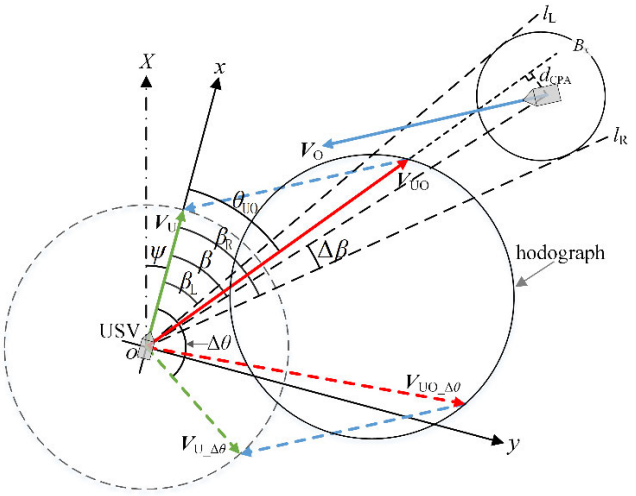

FIGURE 3. Schematic diagram of velocity variables and geometrical relationship between USV and obstacle. θ_{UO} is direction of V_{UO}. If USV continuously rotates $\Delta\theta$ at a constant speed, then hodograph of resulting velocity $V_{U\_\Delta\theta}$ forms circular trajectory. ψ is USV heading. l_L and l_R radiate from USV center and are tangent to perimeter B_X. Their angles are β_L and β_R in oxy. $\Delta\beta$ is deviation angle. d_{CPA} is value of DCPA.

It is assumed that there is a virtual USV with a heading $\Delta\theta$ in oxy at time T. The velocity of this virtual USV is $(v_U, \Delta\theta)$ in oxy, and it is expressed by $\boldsymbol{V}_{U\_\Delta\theta} = v_U e^{i\Delta\theta}$ in ox. The relative velocity $\boldsymbol{V}_{UO\_\Delta\theta} = v_{UO\_\Delta\theta} e^{i\theta_{UO\_\Delta\theta}}$ is determined by

$$\boldsymbol{V}_{UO\_\Delta\theta} = \boldsymbol{V}_{U\_\Delta\theta} - \boldsymbol{V}_O \tag{1}$$

where $v_{UO\_\Delta\theta}$ and $\theta_{UO\_\Delta\theta}$ are the virtual relative speed and direction, respectively. When $\Delta\theta$ is determined, $\theta_{UO\_\Delta\theta}$ can be calculated by taking the four-quadrant inverse tangent of $\boldsymbol{V}_{UO\_\Delta\theta}$. If $\Delta\theta$ makes $\theta_{UO\_\Delta\theta}$ satisfy $d_{CPA} \le r_x$, where $d_{CPA} = d\sin\left(\left|\theta_{UO\_\Delta\theta} - \beta\right|\right)$, then $\Delta\theta$ is defined as an infeasible angle with respect to B_x; otherwise, it is a feasible angle. All infeasible angles constitute the infeasible angle interval $\bar{\boldsymbol{\Psi}}$. Define $\boldsymbol{U}$ as the universal set. The feasible angle interval $\boldsymbol{\Psi}$ is the complementary set of $\bar{\boldsymbol{\Psi}}$, which can be expressed by

$$\boldsymbol{\Psi} = \complement_{\boldsymbol{U}} \bar{\boldsymbol{\Psi}} \tag{2}$$

For a certain perimeter B_x, the condition $d_{CPA} \le r_x$ can be equivalent to another condition $\theta_{UO\_\Delta\theta} \in \boldsymbol{\Phi}$, where $\boldsymbol{\Phi}$ is an angle interval with the value of

$$\boldsymbol{\Phi} = \begin{cases} [\beta_L, \beta_R] & \beta_L < \beta_R \\ (-\pi, \beta_R] \bigcap [\beta_L, \pi] & \beta_L \ge \beta_R \end{cases} \tag{3}$$

TABLE 3. Categories and geometrical relationship legends formed by hodograph and two rays.

Category	Geometrical relationship legends	Description
Cate.1	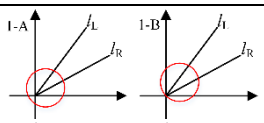	$v_O \le v_U$.
Cate.2	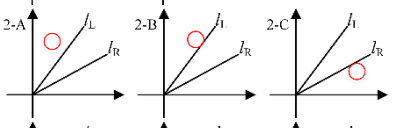	$v_O > v_U$. Hodograph does not intersect with two rays l_L and l_R. No $\theta_{UO\_\Delta\theta}$ is within $\widetilde{\boldsymbol{\Phi}}$. $\widetilde{\boldsymbol{\Phi}}$ is the open interval of $\boldsymbol{\Phi}$.
Cate.3	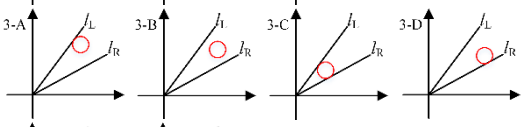	$v_O > v_U$. Hodograph does not intersect with two rays l_L and l_R. All $\theta_{UO\_\Delta\theta}$ are within $\widetilde{\boldsymbol{\Phi}}$.
Cate.4	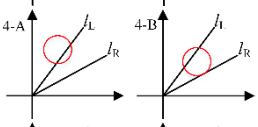	$v_O > v_U$. Hodograph only intersects with l_L.
Cate.5	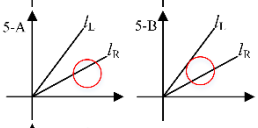	$v_O > v_U$. Hodograph only intersects with l_R.
Cate.6	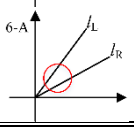	$v_O > v_U$. Hodograph intersects with both l_L and l_R.

This angle interval is between the two boundary rays (l_L and l_R) that radiate from the USV center $\hat{C}$ and tangent to B_x, as shown in Fig. 3. β_L and β_R are the boundary angles calculated by

$$\begin{cases} \beta_L = f_M(\beta - \Delta\beta) \\ \beta_R = f_M(\beta + \Delta\beta) \end{cases} \tag{4}$$

$$\Delta\beta = \sin^{-1}\left(\frac{r}{d}\right), r < d \tag{5}$$

For the perimeter B_x, $r = r_x$. Based on (1), the hodograph of $\boldsymbol{V}_{UO\_\Delta\theta}$ forms a circular trajectory with a continuous rotation of $\Delta\theta$, as shown in Fig. 3. According to the relationship between the hodograph and the two rays l_L and l_R, there are six categories with 14 situations. The legends of the geometric relationships between the hodograph and the two rays l_L and l_R for the different situations are shown in Table 3.

2) CONDITIONS OF ANGLE INTERVALS

$\theta_{UO\_\Delta\theta}$ can be calculated by

$$\theta_{UO\_\Delta\theta}(\Delta\theta) = \text{atan2}\left(\text{Im}\left(\boldsymbol{V}_{UO\_\Delta\theta}\right), \text{Re}\left(\boldsymbol{V}_{UO\_\Delta\theta}\right)\right) \tag{6}$$

where $\text{Re}(\boldsymbol{V})$ and $\text{Im}(\boldsymbol{V})$ represent the real and imaginary parts of $\boldsymbol{V}$, respectively, and $z = \text{atan2}(y, x)$ is the four-quadrant inverse tangent in $\boldsymbol{U}$. Based on (6),

$$\sin\left(\Delta\theta - \theta_{UO\_\Delta\theta}\right) = \delta \sin\left(\theta_O - \theta_{UO\_\Delta\theta}\right) \tag{7}$$

where $\delta = v_O / v_U$. This is a necessary but not sufficient condition of (6).

Based on the legends in Table 3, $\boldsymbol{\Psi}$ and $\bar{\boldsymbol{\Psi}}$ may contain one or two continuous independent subintervals (except $\emptyset$ or $\boldsymbol{U}$) with two or four boundary values. These possible boundary values are denoted by $\Delta\theta_i$, $i = 1, \ldots, 4$. When $\theta_{UO\_\Delta\theta} = \beta_i$, β_i is a given value of

$$\beta_i = f_M(\beta + \text{sign}(i - 2.5)\Delta\beta) \tag{8}$$

the valid $\Delta\theta_i$ can be determined based on (7), which is

$$\Delta\theta_i = f_M\left(\beta_i - (-1)^i \sin^{-1}(\chi_{\sin,i}) + \frac{1 + (-1)^i}{2} f_\pi(\chi_{\sin,i})\right) \tag{9}$$

where $\chi_{\sin,i} = \delta \sin(\theta_O - \beta_i)$, and $f_\pi(x)$ takes π when $x \ge 0$, or takes $-\pi$ when $x < 0$.

The conditions to determine the categories of Cate. $j, j = 1, \ldots, 6$ are denoted by C_j. For Cate.1, there is a unique $\Delta\theta$ value that makes $\theta_{UO\_\Delta\theta} = \beta_L$ and $\theta_{UO\_\Delta\theta} = \beta_R$. Based on (7), condition C_1 should be

$$C_1 = (\delta \le 1) \tag{10}$$

For Cate.$j, j = 2, \ldots, 6$, the condition $\bar{C}_1 = (\delta > 1)$ should be satisfied first. Then, additional conditions $C_{A_j}, j = 2, \ldots, 6$ are used for the further classification of Cate.$j, j = 2, \ldots, 6$.

The $C_{A_j}, j = 2, \ldots, 6$ can be determined based on the geometric relationship between the two boundary rays and an open interval $\tilde{\Phi}_{\theta_{UO\_\Delta\theta}}$. $\tilde{\Phi}_{\theta_{UO\_\Delta\theta}}$ is the open interval of $\boldsymbol{\Phi}_{\theta_{UO\_\Delta\theta}}$, which represents the range of $\theta_{UO\_\Delta\theta}$. $\phi_{\min}$

TABLE 4. Infeasible angle interval results and additional information for different categories.

Category	Condition for calculating $\Delta\theta_i$	Valid $\Delta\theta_i$	Infeasible angle interval $\bar{\boldsymbol{\Psi}}$
Cate.2	/	/	$\bar{\boldsymbol{\Psi}} = \emptyset$
Cate.3	/	/	$\bar{\boldsymbol{\Psi}} = \boldsymbol{U}$
Cate.1	$\theta_{\mathrm{UO\_}\Delta\theta} = \beta_{\mathrm{L}}, \theta_{\mathrm{UO\_}\Delta\theta} = \beta_{\mathrm{R}}$	$\Delta\theta_i, i = 1,3$	$\begin{cases}\kappa_1 = \min(\Delta\theta_i), \kappa_2 = \max(\Delta\theta_i) \\ \theta_{\mathrm{t}} = \theta_{\mathrm{UO\_}\Delta\theta}((\kappa_1+\kappa_2)/2) \\ \bar{\boldsymbol{\Psi}} = \begin{cases}(\kappa_1,\kappa_2) & \theta_{\mathrm{t}} \in \boldsymbol{\Phi} \\ (-\pi,\kappa_1)\cup(\kappa_2,\pi] & \theta_{\mathrm{t}} \notin \boldsymbol{\Phi}\end{cases}\end{cases}$
Cate.4	$\theta_{\mathrm{UO\_}\Delta\theta} = \beta_{\mathrm{L}}$	$\Delta\theta_i, i = 1,2$	
Cate.5	$\theta_{\mathrm{UO\_}\Delta\theta} = \beta_{\mathrm{R}}$	$\Delta\theta_i, i = 3,4$	
Cate.6	$\theta_{\mathrm{UO\_}\Delta\theta} = \beta_{\mathrm{L}}, \theta_{\mathrm{UO\_}\Delta\theta} = \beta_{\mathrm{R}}$	$\Delta\theta_i, i = 1,\ldots,4$	$\begin{cases}\text{Sort } \Delta\theta_i \text{ as } \kappa_1 < \kappa_2 < \kappa_3 < \kappa_4 \\ \theta_{\mathrm{t}} = \theta_{\mathrm{UO\_}\Delta\theta}((\kappa_2+\kappa_3)/2) \\ \bar{\boldsymbol{\Psi}} = \begin{cases}(-\pi,\kappa_1)\cup(\kappa_2,\kappa_3)\cup(\kappa_4,\pi] & \theta_{\mathrm{t}} \in \boldsymbol{\Phi} \\ (\kappa_1,\kappa_2)\cup(\kappa_3,\kappa_4) & \theta_{\mathrm{t}} \notin \boldsymbol{\Phi}\end{cases}\end{cases}$

and $\phi_{\max}$ are the two boundary values of $\boldsymbol{\Phi}_{\theta_{\mathrm{UO\_}\Delta\theta}}$. When $\delta > 1$, there is $\boldsymbol{\Phi}_{\theta_{\mathrm{UO\_}\Delta\theta}} \neq \boldsymbol{U}$, and $\theta_{\mathrm{UO\_}\Delta\theta}$ is continuously differentiable in $\boldsymbol{U}$. Therefore, $\phi_{\min}$ and $\phi_{\max}$ are the unique minimum and maximum extremum of $\theta_{\mathrm{UO\_}\Delta\theta}$, and they can be determined by calculating the two extreme points $\left(\Delta\theta_{\mathrm{ext},m}, \theta_{\mathrm{UO\_}\Delta\theta,m}\right), m = 1, 2$, which are

$$\begin{cases} \Delta\theta_{\mathrm{ext},m} = f_{\mathrm{M}}\left(\theta_{\mathrm{O}} - (-1)^m \cos^{-1}\left(\dfrac{1}{\delta}\right)\right) \\ \theta_{\mathrm{UO\_}\Delta\theta,m} = \theta_{\mathrm{UO\_}\Delta\theta}\left(\Delta\theta_{\mathrm{ext},m}\right) \end{cases} \tag{11}$$

Then, $\phi_{\min} = \min\left(\theta_{\mathrm{UO\_}\Delta\theta,m}\right)$ and $\phi_{\max} = \max\left(\theta_{\mathrm{UO\_}\Delta\theta,m}\right)$, where $m = 1, 2$. The correct interval of the alternative intervals determined by $\phi_{\min}$ and $\phi_{\max}$ should be selected as $\boldsymbol{\Phi}_{\theta_{\mathrm{UO\_}\Delta\theta}}$. Set a temporary variable $\theta_{\mathrm{midT}} = (\phi_{\min} + \phi_{\max})/2$, and let $\theta_{\mathrm{UO\_}\Delta\theta} = \theta_{\mathrm{midT}}$. One $\Delta\theta$ solution of (7) can be calculated by

$$\Delta\theta = \theta_{\mathrm{midT}} + \sin^{-1}\left(\delta \sin\left(\theta_{\mathrm{O}} - \theta_{\mathrm{midT}}\right)\right) \tag{12}$$

This calculated $\Delta\theta$ is used as the independent variable of (6) to determine a new $\theta_{\mathrm{UO\_}\Delta\theta}$, which is denoted by θ_{mid}. If $\theta_{\mathrm{mid}} = \theta_{\mathrm{midT}}$, then $\theta_{\mathrm{midT}} \in \boldsymbol{\Phi}_{\theta_{\mathrm{UO\_}\Delta\theta}}$; otherwise, $\theta_{\mathrm{midT}} \notin \boldsymbol{\Phi}_{\theta_{\mathrm{UO\_}\Delta\theta}}$. Therefore, $\boldsymbol{\Phi}_{\theta_{\mathrm{UO\_}\Delta\theta}}$ takes

$$\boldsymbol{\Phi}_{\theta_{\mathrm{UO\_}\Delta\theta}} = \begin{cases} [\phi_{\min}, \phi_{\max}] & \theta_{\mathrm{mid}} = \theta_{\mathrm{midT}} \\ \left(-\pi, \phi_{\min}\right] \bigcap [\phi_{\max}, \pi] & \theta_{\mathrm{mid}} \neq \theta_{\mathrm{midT}}, \end{cases} \tag{13}$$

Finally, $C_{\mathrm{A}_j}, j = 2, \ldots, 6$ can be determined by

$$\begin{cases} C_{\mathrm{A}_2} = \left(\tilde{\boldsymbol{\Phi}}_{\theta_{\mathrm{UO\_}\Delta\theta}} \bigcap \tilde{\boldsymbol{\Phi}} \equiv \emptyset\right) \\ C_{\mathrm{A}_3} = \left(\tilde{\boldsymbol{\Phi}}_{\theta_{\mathrm{UO\_}\Delta\theta}} \bigcap \tilde{\boldsymbol{\Phi}} \equiv \tilde{\boldsymbol{\Phi}}_{\theta_{\mathrm{UO\_}\Delta\theta}}\right) \\ C_{\mathrm{A}_4} = \left(\beta_{\mathrm{L}} \in \tilde{\boldsymbol{\Phi}}_{\theta_{\mathrm{UO\_}\Delta\theta}}\right) \& \left(\beta_{\mathrm{R}} \notin \tilde{\boldsymbol{\Phi}}_{\theta_{\mathrm{UO\_}\Delta\theta}}\right) \\ C_{\mathrm{A}_5} = \left(\beta_{\mathrm{L}} \notin \tilde{\boldsymbol{\Phi}}_{\theta_{\mathrm{UO\_}\Delta\theta}}\right) \& \left(\beta_{\mathrm{R}} \in \tilde{\boldsymbol{\Phi}}_{\theta_{\mathrm{UO\_}\Delta\theta}}\right) \\ C_{\mathrm{A}_6} = \left(\beta_{\mathrm{L}} \in \tilde{\boldsymbol{\Phi}}_{\theta_{\mathrm{UO\_}\Delta\theta}}\right) \& \left(\beta_{\mathrm{R}} \in \tilde{\boldsymbol{\Phi}}_{\theta_{\mathrm{UO\_}\Delta\theta}}\right) \end{cases} \tag{14}$$

where $\tilde{\boldsymbol{\Phi}}$ is the open interval of $\boldsymbol{\Phi}$. The final classification conditions for Cate.j, $j = 2, \ldots, 6$ are $C_j = \bar{C}_1 \,\&\, C_{\mathrm{A}_j}$. One and only one condition of $C_{\mathrm{A}_j}, j = 1, \ldots, 6$ can be used to determine the categories of $\boldsymbol{\Psi}$ and $\bar{\boldsymbol{\Psi}}$.

3) RESULTS OF ANGLE INTERVALS

When the category is known, $\bar{\boldsymbol{\Psi}}$ can be determined based on the category and the additional valid $\Delta\theta_i, i = 1, \ldots, 4$. The results for Cate.2 and Cate.3 are $\emptyset$ and $\boldsymbol{U}$, respectively. There are two valid $\Delta\theta_i$ values for Cate.1, Cate.4, and Cate.5, with different given conditions, and the $\bar{\boldsymbol{\Psi}}$ values of these three categories have the same form. For Cate.6, there are four valid $\Delta\theta_i$ values. The results of $\bar{\boldsymbol{\Psi}}$ and the additional information are shown in Table 4.

When there are multiple obstacles, $\bar{\boldsymbol{\Psi}}$ is the union of $\bar{\boldsymbol{\Psi}}_i$, that is,

$$\bar{\boldsymbol{\Psi}} = \left\{\theta \,|\, \theta \in \bigcup_{i=1}^{N} \bar{\boldsymbol{\Psi}}_i\right\} \tag{15}$$

where $\bar{\Psi}_i$ is the infeasible angle interval of the i^{th} obstacle, and N is the number of obstacles.

B. COLREGS SELECTION

There is an additional constraint for the feasible angle interval $\boldsymbol{\Psi}$ when COLREGs are considered. Rules 13 to 15 define three encounter situations, including overtaking, head-on, and crossing situations [18].

Based on the relative locations between the USV and the encounter vessel, we divide the overtaking situation (Rule 13) into a USV-behind-overtaking situation and USV-ahead-overtaking situation. When the USV is behind and overtakes another vessel, it is the USV-behind-overtaking situation, and the USV is a give-way vessel that is directed to keep out of way of the encounter vessel [18]. When the USV is ahead and going to be overtaken by another vessel, it is the USV-ahead-overtaking situation, and the USV is the stand-on vessel that keeps its course and speed. Based on COLREGs, the USV shall take early and substantial action to keep out of the way of the other vessel when the USV is a give-way vessel [18]. COLREGs do not define a detailed action for the USV to give way in the overtaking situation. Therefore, an action with a right turn is adopted in the proposed algorithm.

In the head-on situation (Rule 14), both the USV and the encounter vessel are give-way vessels, and each shall alter

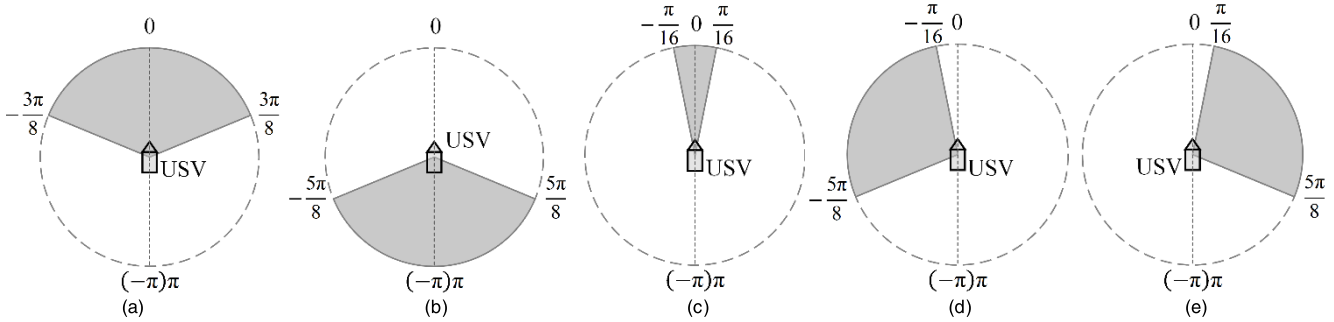

FIGURE 4. Quantitative definitions for different encounter situations. Gray areas represent range of relative direction $\theta_{UO\_\Delta\theta}$. (a) USV-behind-overtaking situation, (b) USV-ahead-overtaking situation, (c) head-on situation, (d) left-crossing situation, and (e) right-crossing situation.

their own course to starboard [18]. Similar to the overtaking situation, the crossing situation (Rule 15) is further divided into a left-crossing situation and a right-crossing situation. In the left-crossing situation, the encounter vessel is on the port side of the USV, and the USV is the stand-on vessel. In the right-crossing situation, the USV has another vessel on its starboard side, and it is the give-way vessel that shall keep out of the way and shall avoid crossing ahead of the other vessel when the circumstance requires it [18].

The definitions for the head-on and crossing situations are not defined quantitatively in COLREGs. There are some differences in the quantitative definitions of these encounter situations in different studies [28]–[30]. A compromise definition is selected in this study. The detailed quantitative definitions are shown in Fig. 4, in which the gray areas represent the range of the relative direction $\theta_{UO\_\Delta\theta}$. The conditions for different encounter situations and corresponding required roles played by the USV are shown in Table 5.

TABLE 5. Conditions for different encounter situations and corresponding required roles played by USV.

Situation	Condition	USV role
USV-behind-overtaking	$\begin{cases}\theta_{UO\_\Delta\theta} \in (-3\pi/8, 3\pi/8) \\ \boldsymbol{V}_U \cdot \boldsymbol{V}_O > 0 \\ v_U > v_O\end{cases}$	Give-way
USV-ahead-overtaking	$\begin{cases}\theta_{UO} \in (-\pi, -5\pi/8) \cap (5\pi/8, \pi) \\ \boldsymbol{V}_U \cdot \boldsymbol{V}_O > 0 \\ v_U < v_O\end{cases}$	Stand-on
Head-on	$\begin{cases}\theta_{UO\_\Delta\theta} \in [-\pi/16, \pi/16] \\ \boldsymbol{V}_U \cdot \boldsymbol{V}_O < 0\end{cases}$	Give-way
Left-crossing	$\theta_{UO\_\Delta\theta} \in [-5\pi/8, -\pi/16)$	Stand-on
Right-crossing	$\theta_{UO\_\Delta\theta} \in (\pi/16, 5\pi/8]$	Give-way

Based on the above introduction about the different situations and the requested actions of the USV, a timely and sufficient steering action with a right turn is available when the USV is a give-way vessel. When the USV is a stand-on vessel, it will maintain its course and speed based on COLREGs. However, most USVs are small and difficult to detect by other vessels in many situations. Therefore, the other give-way vessels may not take valid actions to avoid collision. In such situations, the USV shall take action to avoid collision. For the USV-ahead-overtaking situation, it may still work by turning right with a substantial angle in time. The action to alter the course to port is not suggested by the COLREGs in the left-crossing situation [18]. Therefore, the USV should also take action by turning right to avoid collision if the other give-way vessel does not take the appropriate action. Whether the USV should take action to avoid collision depends on the steering occasion introduced in the next section.

Based on the above discussion, when the USV should take action to avoid collision considering COLREGs, $\boldsymbol{\Psi}$ is limited to $\boldsymbol{\Psi}_{\text{COLREGs}} = (0, \pi]$. In other words, the final infeasible angle interval $\bar{\boldsymbol{\Psi}}_{\text{alg}}$ for the algorithm is adjusted to

$$\bar{\boldsymbol{\Psi}}_{\text{alg}} = \bar{\boldsymbol{\Psi}} \bigcup \bar{\boldsymbol{\Psi}}_{\text{COLREGs}} \tag{16}$$

where $\bar{\Psi}_{\text{COLREGs}}$ is a complementary set of $\boldsymbol{\Psi}_{\text{COLREGs}}$ in the complete set $\boldsymbol{U}$ and can be expressed by

$$\bar{\boldsymbol{\Psi}}_{\text{COLREGs}} = \complement_{\boldsymbol{U}} \boldsymbol{\Psi}_{\text{COLREGs}} = (-\pi, 0] \tag{17}$$

If no COLREGs are considered, then $\bar{\boldsymbol{\Psi}}_{\text{alg}} = \bar{=}\boldsymbol{\Psi}$. The final feasible angle interval $\boldsymbol{\Psi}_{\text{alg}}$ for the algorithm can be determined by $\boldsymbol{\Psi}_{\text{alg}} = \complement_{\boldsymbol{U}} \bar{\boldsymbol{\Psi}}_{\text{alg}}$.

C. STEERING OCCASION WITH RESPECT TO OBSTACLES

According to Rule 8 of COLREGs, it is better to avoid a collision as soon as possible when a USV detects a possible collision with a moving vessel [18]. Unfortunately, deviations exist in most information about detected obstacles, and they are much higher when the obstacles are far from the USV with high probability. There may even be false obstacles in some environments. Therefore, an immediate avoidance action will not be a good choice in many actual situations. In order to reduce the influence of these factors, a steering occasion that can be equivalent to a safe distance interval is adopted for collision avoidance.

1) MARGINAL STEERING ANGULAR VELOCITIES

For a valid virtual USV heading $\Delta\theta_i$, there exists a minimum angular velocity for the USV collision avoidance, which is defined as the marginal steering angular velocity $\omega_i(d)$. Except for Cate.2 and Cate.3, $\Delta\theta_i, i = 1, \ldots, 4$ in other

categories are related to the relative distance d, which are

$$\Delta\theta_i(d) = f_{\mathrm{M}}\begin{pmatrix}\beta_i(d) - (-1)^i \sin^{-1}\left(\chi_{\sin,i}(d)\right)\\ +\frac{1+(-1)^i}{2} f_\pi\left(\chi_{\sin,i}(d)\right)\end{pmatrix} \quad (18)$$

where

$$\beta_i(d) = f_{\mathrm{M}}\begin{pmatrix}\theta_{\mathrm{UO}} + \mathrm{sign}(\beta - \theta_{\mathrm{UO}}) f_{\mathrm{asin}}(d_{\mathrm{CPA}}, d)\\ +\mathrm{sign}(i-2.5) f_{\mathrm{asin}}(r, d)\end{pmatrix} \quad (19)$$

$$\chi_{\sin,i}(d) = \delta \sin(\theta_{\mathrm{O}} - \beta_i(d)), \quad (20)$$

$$f_{\mathrm{asin}}(x,y) = \sin^{-1}\left(\frac{x}{y}\right), \quad (21)$$

θ_{UO}, θ_{O}, β, and d_{CPA} are the values at time T, and r is the corresponding r_x with respect to B_x.

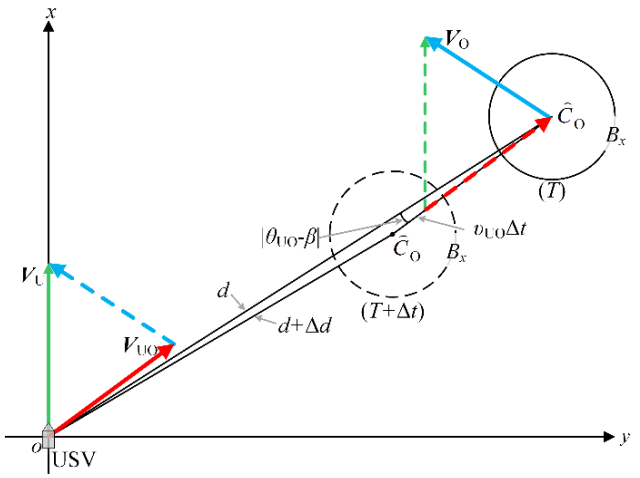

FIGURE 5. Geometric relationship between USV and obstacles at time T and time $T + \Delta t$. $d + \Delta d$ is relative distance between USV and obstacle at time $T + \Delta t$.

The geometric relationship between the USV and obstacles at time T and $T + \Delta t$ is shown in Fig. 5. Based on the triangle cosine theorem,

$$(d+\Delta d)^2 = (v_{\mathrm{UO}}\Delta t)^2 + d^2 - 2d(v_{\mathrm{UO}}\Delta t)\cos(\theta_{\mathrm{UO}} - \beta) \quad (22)$$

Based on (22), $\omega_i(d)$ can be calculated by

$$\begin{aligned}\omega_i(d) &= \lim_{\Delta t \to 0^+} \frac{\Delta\theta_i(d+\Delta d) - \Delta\theta i(d)}{\Delta t}\\ &= -v_{\mathrm{U}}\mathrm{COS}(\theta_{\mathrm{UO}} - \beta) f_{x,i}(d)\beta'_i(d)\end{aligned} \quad (23)$$

where

$$f_{\chi,i}(d) = 1 + (-1)^i \frac{\chi_{\cos,i}(d)}{\sqrt{1-\chi^2_{\sin,i}(d)}} \quad (24)$$

$$\begin{aligned}\beta'_i(d) &= \mathrm{sign}(i-2.5) f_{\mathrm{dasin}}(r,d)\\ &\quad +\mathrm{sign}(\beta - \theta_{\mathrm{UO}}) f_{\mathrm{dasin}}(d_{\mathrm{CPA}}, d)\end{aligned} \quad (25)$$

$$\chi_{\cos,i}(d) = \delta\cos(\theta_{\mathrm{O}} - \beta_i(d)), \quad (26)$$

$$f_{\mathrm{dasin}}(x,y) = -\frac{x}{y\sqrt{y^2-x^2}} \quad (27)$$

In a possible collision situation $d_{\mathrm{CPA}} \le r$, $|\omega_i(d)|$ increases with decreasing d, except for the only condition that satisfies $\delta = 1$ and $\chi_{\cos,i}(d) \ge 0$. For this condition, $\omega_i(d) \equiv 0$.

2) STEERING OCCASION

Every USV has constraints on its dynamic performance such as maximum speed, acceleration, and angular velocity. The steering occasion is mainly related to the angular velocity constraint of a USV. For every valid $\omega_i(d)$, it can be equivalent to a relative distance d_i value based on the monotonicity of $|\omega_i(d)|$. Therefore, the steering occasion is designed to be related to a distance interval $\boldsymbol{D}_{\mathrm{SO}} = [d_{\mathrm{SO\_s}}, d_{\mathrm{SO\_l}}]$, where $d_{\mathrm{SO\_s}}$ and $d_{\mathrm{SO\_l}}$ are the short-distance and long-distance boundaries, respectively.

The short-distance boundary $d_{\mathrm{SO\_s}}$ is important for collision avoidance by altering the course. The d_i value, which corresponds to $\omega_{i,\mathrm{S}}(d_i) = \omega_{\max}/2$, is selected as a candidate $d_{\mathrm{SO\_s},i}$, where $\omega_{\max}$ is the maximal angle velocity of a USV, and $\omega_{i,\mathrm{S}}(d_i)$ are the $\omega_i(d_i)$ values with respect to the perimeter B_{S}. The analytical solution of $d_{\mathrm{SO\_s},i}$ is difficult to obtain. A discrete numerical solution was adopted to approximate $d_{\mathrm{SO\_s},i}$. Then, $d_{\mathrm{SO\_s}}$ takes the largest value of all valid $d_{\mathrm{SO\_s},i}$. The long-distance boundary $d_{\mathrm{SO\_l}}$ is set to $d_{\mathrm{SO\_l}} = d_{\mathrm{SO\_s}} + \Delta d_{\mathrm{SO}}$, where Δd_{SO} is the setting distance.

Finally, the steering occasion is determined by comparing d and $d_{\mathrm{SO\_l}}$. If $d > d_{\mathrm{SO,l}}$, then the steering occasion is not satisfied, and the contribution of $\bar{\boldsymbol{\Psi}}$ caused by a dynamic obstacle is ignored. Otherwise, the USV should take a steering action to avoid possible collisions.

D. NAVIGATION WAYPOINT MODEL

A USV path commonly consists of multiple waypoints. The mature waypoint navigation technology has been applied well to USV control. Therefore, a navigation waypoint model is used for the USV to avoid collision. In this model, an updatable NWP is set for the entire navigation of a USV. Two types of waypoints are set for navigation: the goal waypoint P_{G} and the temporary waypoint P_i, which is determined by a real-time optimal orientation angle and a setting distance.

1) NAVIGATION WAYPOINT

When a USV navigates to a certain waypoint of an original path, this waypoint is treated as the current P_{G}. It is set as the NWP when the USV can navigate to it directly without a collision. Otherwise, an updatable P_i is set as the NWP. When a P_i needs to be set or updated, there is

$$\begin{cases} x_{P_i} = x_{\hat{C}} + d_{P_i}\cos(\theta_{\mathrm{opt}} + \psi)\\ y_{P_i} = y_{\hat{C}} + d_{P_i}\sin(\theta_{\mathrm{opt}} + \psi),\end{cases} \quad (28)$$

where $(x_{\hat{C}}, y_{\hat{C}})$ and (x_{P_i}, y_{P_i}) are locations of the USV and P_i, θ_{opt} is the real-time optimal orientation angle, and d_{P_i} is the setting distance.

2) REAL-TIME OPTIMUM ORIENTATION ANGLE

θ_{opt} is used to evaluate whether the NWP needs to be updated and to determine P_{i+1} when necessary. The optimization objective function $F_{\text{opt}}(\theta)$ is designed by a weighting deviation degree combination of the orientation angle θ with respect to the goal orientation and obstacles:

$$F_{\text{opt}}(\theta) = \lambda_1 F_{\text{goal}}(\theta) + \lambda_2 F_{\text{safe}}(\theta), \tag{29}$$

$$\theta \notin \bar{\boldsymbol{\Psi}}_{\text{alg}} \tag{30}$$

where λ_1 and λ_2 are weighted values satisfying $\lambda_1 + \lambda_2 = 1$. $F_{\text{goal}}(\theta)$ is the degree of proximity to the goal orientation, and $F_{\text{safe}}(\theta)$ is the combination of deviation degrees to infeasible angle intervals:

$$F_{\text{goal}}(\theta) = 1 - \frac{|\theta_{\text{G}} - \theta|}{\pi} \tag{31}$$

$$F_{\text{safe}}(\theta) = \frac{1}{N'} \sum_{j=1}^{N}{}' \frac{\left|\theta - \theta_{\bar{\boldsymbol{\Psi}}_{\text{alg},j}}\right|}{\pi} \tag{32}$$

where θ_{G} is the goal orientation, N' is the number of valid independent infeasible angle subintervals, and $\theta_{\bar{\boldsymbol{\Psi}}_{\text{alg},j}}$ is the center angle of the corresponding independent subinterval. When considering COLREGs, $\bar{\boldsymbol{\Psi}}_{\text{alg}}$ takes the result of (16); otherwise, $\bar{\boldsymbol{\Psi}}_{\text{alg}} = \bar{\boldsymbol{\Psi}}$.

Cate.2 is safe for a USV, and no action is taken for collision avoidance. Cate.3 can no longer achieve safe collision avoidance by using steering alone. In such situations, other methods to alter the USV speed and heading simultaneously for collision avoidance can be used, but they are not discussed in this paper. For other categories, there may be one or two continuous independent infeasible angle subintervals for one obstacle. $N' = N_1 + 2N_2$, where N_1 and N_2 are the numbers of obstacles for these two situations. The corresponding θ that maximizes $F_{\text{opt}}(\theta)$ is selected as θ_{opt}.

IV. LOCAL COLLISION AVOIDANCE USING FSM

Local collision avoidance based on waypoint navigation mainly includes the processes of NWP navigation and NWP updates. To design the processes with suitable elements of FSM, collision avoidance can be effectively implemented using FSM.

The designed FSM is recorded as $\mathcal{F} = (\mathcal{S}, \mathcal{C}, \mathcal{T}, S_0, S_{\text{g}})$. $\mathcal{S}$ is a finite set of discrete states. Several states have corresponding actions for collision avoidance. $\mathcal{C}$ is a finite set of conditions for transitions between states. $\mathcal{T}$ is a finite set of transition relations. In addition to the state transition from one state to another, there are self-state transitions. S_0 and S_{g} are the start and goal states, respectively, where $S_0, S_{\text{g}} \subset \mathcal{S}$. The main purpose of the FSM design is to determine $\mathcal{S}, \mathcal{C}, \mathcal{T}$, and the state transition diagram.

In addition to the start, goal, and emergency states, two different navigation states and two NWP update states for P_{G} and P_i are designed. Therefore, $\mathcal{S} = \{S_0, \ldots, S_6\}$, where $S_{\text{g}} = S_6$. The detailed state definitions and corresponding actions are shown in Table 6.

TABLE 6. Finite states and corresponding actions of designed FSM.

State	Description	Action
S_0	Start state	Initialize parameters
S_1	P_{G} navigation state	Navigate USV to P_{G}
S_2	P_i navigation state	Navigate USV to P_i
S_3	P_{G} update state	Update NWP from P_i to P_{G}
S_4	P_{i+1} update state	Update NWP from P_i or P_{G} to P_{i+1}
S_5	Emergency state	Perform speed and course alteration
S_6	Goal state	Finish the mission

A state transition $T_{i\to j} \subset \mathcal{T}$ indicate a transition from the current state S_i to the next state S_j. When $i = j$, it is a self-state transition. Considering the collision avoidance process, $\mathcal{T}$ is designed as follows:

$$\mathcal{T} = \left\{ \begin{array}{l} \mathcal{T}_{0\to1}, \mathcal{T}_{1\to1}, \mathcal{T}_{1\to4}, \mathcal{T}_{1\to5}, \mathcal{T}_{1\to6}, \mathcal{T}_{2\to2}, \mathcal{T}_{2\to3}, \\ \mathcal{T}_{2\to4}, \mathcal{T}_{2\to5}, \mathcal{T}_{2\to6}, \mathcal{T}_{3\to1}, \mathcal{T}_{4\to2}, \mathcal{T}_{5\to0} \end{array} \right\} \tag{33}$$

$\mathcal{C}$ and $\mathcal{S}$ jointly determine $\mathcal{T}$. The corresponding condition $C_{i\to j} \subset \mathcal{C}$ for $T_{i\to j}$ can be determined by combining the relevant basic conditions $C_{\text{B}_k}, k = 0, 1, 2, \ldots$. The detailed C_{B_k} conditions are shown in Table 7, and the relevant parameters are listed in Table 8. The values of $C_{\text{B}_k}, k = 1, 2, \ldots$ are ordered by priority. If the k^{th} condition is satisfied, then set $C_{\text{B}_k} = \text{C}_{\text{B}_k}$; otherwise, set $C_{\text{B}_k} = \bar{C}_{\text{B}_k}$. The detailed combinations for $C_{i\to j}$ are shown in Table 9. $\bar{C}_{\text{B}_1} \cdots \bar{C}_{\text{B}_{k-1}} \text{C}_{\text{B}_k}, k \geq 2$ means that C_{B_1} to $C_{\text{B}_{k-1}}$ are not satisfied and C_{B_k} is satisfied, while $\bar{C}_{\text{B}_1} \cdots \bar{C}_{\text{B}_k}, k \geq 2$ represents that no C_{B_1} to C_{B_k} are satisfied.

TABLE 7. Basic conditions with corresponding information.

Basic condition	Mathematical expression	Description
C_{B_0}	None	Without any conditions
C_{B_1}	$\bar{\boldsymbol{\Psi}}_{\text{alg\_S}} \equiv \boldsymbol{U}$	Emergency situation
C_{B_2}	$d_{\tilde{C}P_{\text{G}}} \leq \varepsilon_d$	USV reaches P_{G}
C_{B_3}	$\boldsymbol{\Psi}_{\text{G}} \cap \bar{\boldsymbol{\Psi}}_{\text{alg\_S}} \equiv \emptyset$	No infeasible angle intervals in $\boldsymbol{\Psi}_{\text{G}}$
C_{B_4}	$d \in [D_{\text{SO\_s}}, D_{\text{SO\_l}}]$	USV satisfies steering occasion for a dynamic obstacle first time
C_{B_5}	$d_{\tilde{C}P_i} \leq \varepsilon_d$	USV reaches P_i
C_{B_6}	$\left\lvert f_{\text{M}}(\theta_{\text{opt}} - \theta_{\text{N}}) \right\rvert > \varepsilon_\theta$	Difference between θ_{opt} and θ_{N} is larger than threshold ε_θ

TABLE 8. Relevant parameter definitions in Table 7.

Parameter	Definition
$d_{\tilde{C}P_{\text{G}}}$	Distance between USV and P_{G}
$d_{\tilde{C}P_i}$	Distance between USV and P_i
ε_d	Allowable distance error
ε_θ	Allowable angle error
θ_{N}	Real-time expected orientation angle of P_i
$\boldsymbol{\Psi}_{\text{G}}$	Angle interval between USV heading and θ_{G} in oxy
$\bar{\boldsymbol{\Psi}}_{\text{alg\_S}}$	$\bar{\boldsymbol{\Psi}}_{\text{alg}}$ determined based on perimeter B_{S}

TABLE 9. Basic condition combinations for transition conditions.

Transition condition	Basic condition combination
$C_{0\to1}$	C_{B_0}
$C_{1\to1}$	$\overline{C}_{B_1}\overline{C}_{B_2}C_{B_3}$
$C_{1\to4}$	$\overline{C}_{B_1}\overline{C}_{B_2}\overline{C}_{B_3}$
$C_{1\to5}$	C_{B_1}
$C_{1\to6}$	$\overline{C}_{B_1}C_{B_2}$
$C_{2\to2}$	$\overline{C}_{B_1}\cdots\overline{C}_{B_6}$
$C_{2\to3}$	$\overline{C}_{B_1}\overline{C}_{B_2}C_{B_3}$
$C_{2\to4}$	$\overline{C}_{B_1}\cdots\overline{C}_{B_{k-1}}C_{B_k}, k=4,5,6$
$C_{2\to5}$	C_{B_1}
$C_{2\to6}$	$\overline{C}_{B_1}C_{B_2}$
$C_{3\to1}$	C_{B_0}
$C_{4\to2}$	C_{B_0}
$C_{5\to0}$	$\overline{C}_{B_1}$

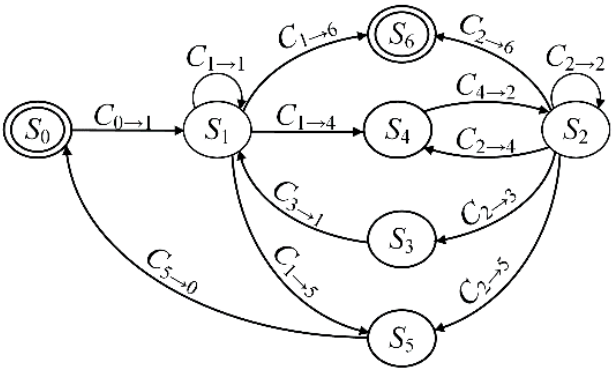

FIGURE 6. State transition diagram of the designed FSM.

The state transition diagram can be designed as shown in Fig. 6. The single/double circle with state S_i represents a state with its action. The arrow represents the transition from S_i to S_j. Based on the diagram, a state modification that includes adding, deleting, or changing a state will only influence the state itself and the relevant conditions. Therefore, the FSM is easily modified when the algorithm is improved.

V. SIMULATION RESULTS AND DISCUSSIONS

A. SIMULATION ENVIRONMENTS AND THE USV

A virtual obstacle module is designed to simulate an environment with both static and dynamic obstacles. In this module, obstacles are created with rand positions and radii. Gaussian noises are added to obstacle positions to simulate the detected position errors of actual obstacles as far as possible. The estimated position $\left(\tilde{x}_{O_i}, \tilde{y}_{O_i}\right)$ for the simulation satisfies

$$\left(\tilde{x}_{O_i}, \tilde{y}_{O_i}\right) \sim N\left(\bar{x}_{O_i}, \bar{y}_{O_i}, \sigma^2_{\tilde{x}_{O_i}}, \sigma^2_{\tilde{y}_{O_i}}, \rho_{O_i}\right) \tag{34}$$

where $\left(\bar{x}_{O_i}, \bar{y}_{O_i}\right)$ is the position of the i^{th} obstacle. The standard deviations $\sigma_{\tilde{x}_{O_i}}$ and$\sigma_{\tilde{y}_{O_i}}$ are assumed to have a linear relationship with distance:

$$\sigma_{\tilde{x}_{O_i}} = \sigma_{\tilde{y}_{O,i}} = \frac{1}{3}\left(\Delta d_0 + \frac{d_i - r_{O_i}}{d_{\text{det}}}\Delta d_1\right) \tag{35}$$

FIGURE 7. "JiuHang490" USV.

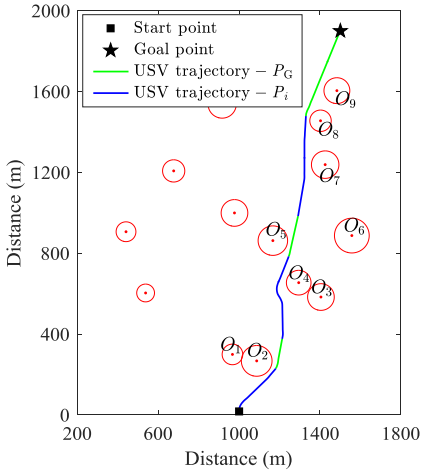

FIGURE 8. Simulation environment with static obstacles and simulation trajectory through obstacle area. Red circles represent static obstacles. Their radii equal their corresponding r_P. O_1 to O_9 represent obstacles detected in navigation of USV. Green and blue portions of trajectory are navigated by goal waypoint P_G and temporary waypoints P_i respectively.

where Δd_0 and Δd_1 are the distance deviations. d_i is the distance between the USV and the i^{th} obstacle. r_{O_i} is the radius of the i^{th} obstacle. d_{det} is the detection distance, which is

$$d_{\text{det}} = d_{\text{detB}} + \text{rand}\,(1) * d_{\text{detF}} \tag{36}$$

where d_{detB} and d_{detF} are the base detection distance and the fluctuant distance, respectively; and rand (1) takes a rand value between 0 and 1. The correlation coefficient always takes $\rho_{O_i} = 0$. For a dynamic obstacle, the corresponding noises are also added to the speed and direction. The estimated speed and direction of the j^{th} dynamic obstacle $\tilde{v}_{O_j}$ and $\tilde{\theta}_{O_j}$ fluctuate and satisfy

$$\tilde{v}_{O_j} \sim N\left(\bar{v}_{O_j}, \bar{v}_{O_j}/10\right) \tag{37}$$

$$\tilde{\theta}_{O_j} = \bar{\theta}_{O_j} + (m-3)\,\Delta_\theta \tag{38}$$

where $\bar{v}_{O_j}$ and $\bar{\theta}_{O_j}$ are the base speed and direction in OXY, respectively; m is an integer between 1 and 5 with a discrete

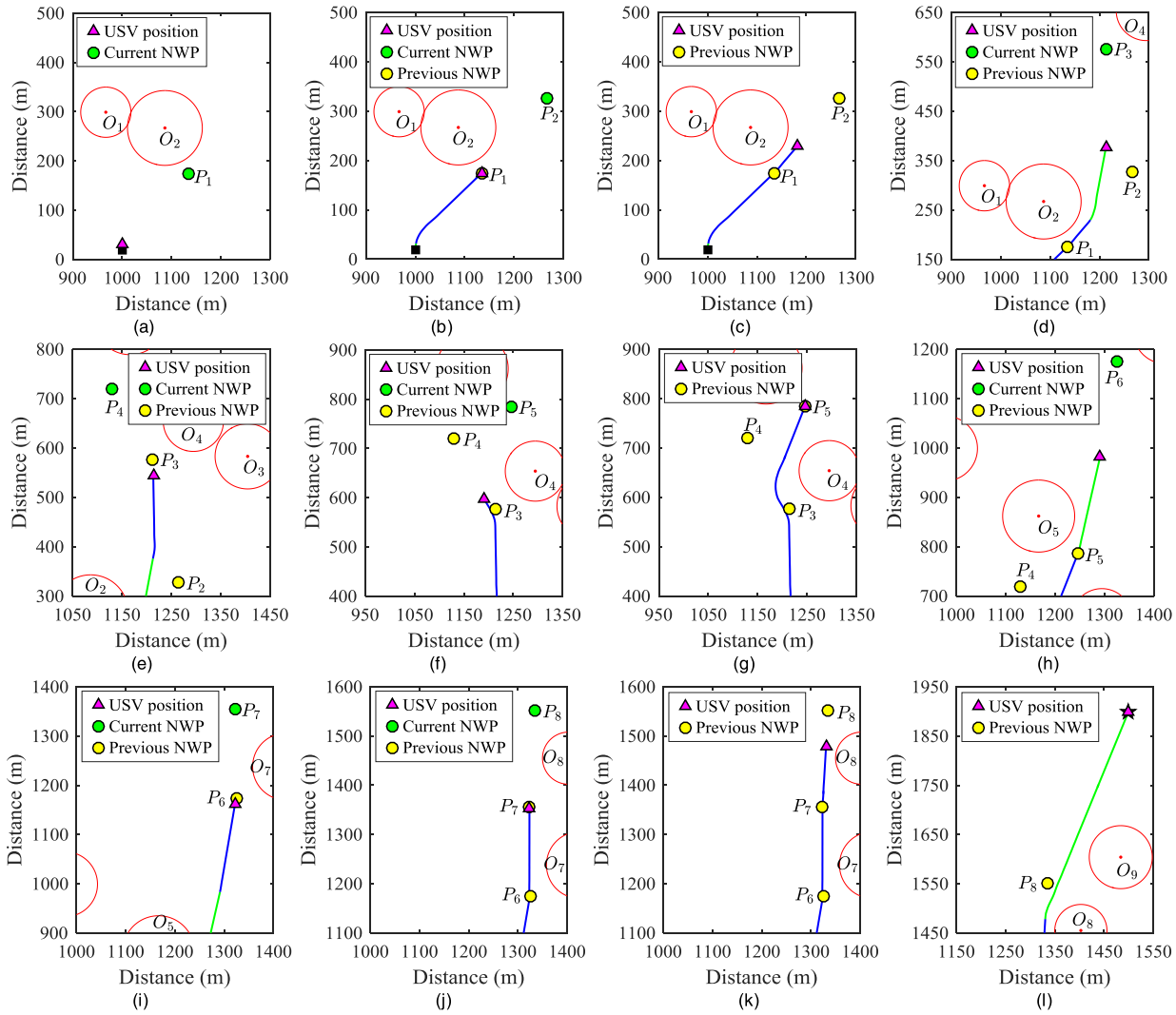

FIGURE 9. USV navigation and NWP update progress in static obstacle environment. (a) NWP is set to temporary waypoint P_1 at time T_1. (b) USV reaches P_1, and NWP updates to P_2 at T_2. (c) NWP updates to P_G at T_3. (d) New obstacles are detected, and NWP updates to P_3 at T_4. (e) NWP updates to P_4 at T_5. (f) NWP updates to P_5 to navigate USV through gap between obstacles at T_6. (g) USV reaches P_5, and NWP updates to P_G at T_7. (h) NWP updates to P_6 at T_8. (i) NWP updates to P_7 at T_9. (j) USV reaches P_5, and NWP updates to P_G at T_{10}. (k) NWP updates to P_G at T_{11}. (l) USV reaches P_G at T_{12}.

probability $P(m)$; and Δ_θ is the angle deviation. Static obstacles are stable when they are produced at the beginning of the simulation. Dynamic obstacles are generated randomly during each period. The ones within the detected range of a USV will persist and be updated based on its basic motion, while the others will be removed.

The basic parameters are listed in Table 10 and are designed for simulation of the "JiuHang490" USV, as shown in Fig. 7 [31]. A particle model with dynamic performance constraints for the USV was used to simulate an actual situation. Using these common parameters, four types of simulation cases are conducted to validate the feasibility and validity of the proposed algorithm for different purposes. It is assumed that all obstacles are unknown before the navigation of the USV. The simulations are performed on a computer with a configuration of i7-6700 CPU and 12 GB RAM.

TABLE 10. Basic simulation parameters.

Parameters	Values
v_U	6 m/s
L_U	5 m
ω_{max}	5°/s
d_{P_i}	200 m
Δd_0	5 m
Δd_1	5 m
d_{detB}	300 m
d_{detF}	30 m
$P(m)$	{0.1,0.2,0.4,0.2,0.1}
Δ_θ	1°

The operating system is a 64-bit Win7, and the algorithm is executed in the MATLAB environment. The execution time of the algorithm in each cycle is completely in real time for the USV control cycle.

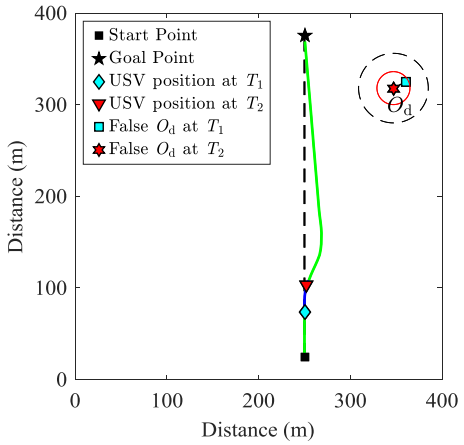

FIGURE 10. Collision avoidance case with false obstacle O_d. Solid and dashed circles around O_d represent perimeters B_P and B_S. Solid trajectory composed of green and blue portions is acquired by algorithm without adopting steering occasion, and dashed trajectory is acquired by algorithm adopting steering occasion.

B. COLLISION AVOIDANCE IN STATIC OBSTACLE ENVIRONMENT

For USV missions in complex marine environments, there may be unknown obstacles such as small reefs on the planned global path. Therefore, the USV should have the ability to avoid such obstacles. Although the proposed algorithm is mainly for dynamic obstacles, it is also effective in environments with static obstacles.

Fig. 8 shows a static obstacle environment and a typical simulated trajectory through the obstacle area. The start and goal positions are (1000 m, 20 m) and (1500 m, 1900 m). More information about the USV navigation and NWP update progress is shown in Fig. 9.

When the USV sails from the start position, NWP is first set to the goal waypoint P_G. Then, the USV detects O_1 and O_2 at time T_1, and a temporary waypoint P_1 is set as the NWP to navigate the USV bypass the two obstacles, as shown in Fig. 9(a). As the USV sails toward P_1, the influence of obstacles still exists. The NWP does not update until the USV reaches P_1 at T_2, and then it updates to P_2, as shown in Fig. 9(b). In Fig. 9(c), the influence of O_1 and O_2 is negligible at T_3, and no other obstacles are detected. Therefore, the NWP is set to P_G again, and the USV turns toward it directly. When O_3 and O_4 are detected at T_4, the NWP updates to P_3 to navigate the USV, as shown in Fig. 9(d). Before the USV reaches P_3, O_5 is detected at T_5, and the USV turns towards the new P_4 [see Fig. 9(e)]. After sailing for a while, the USV finds a better evaluated path and updates the NWP to P_5 to sail through the gap at T_6, as shown in Fig. 9(f). When the USV reaches P_5 at T_7, the NWP is updated again [see Fig. 9(g)]. Although O_5 and O_6 are within the detection range of the USV, their influence can be ignored, and the USV turns to P_G again. Then, O_7 is detected at T_8, and this is dangerous for the USV. Therefore, the NWP updates to P_6 to navigate the USV, as shown in Fig. 9(h). When the USV detects O_8 before the USV reaches P_6 at T_9, the NWP updates to P_7 to avoid possible collisions with O_8, as shown in Fig. 9(i). When the USV reaches P_7 at T_{10}, the NWP updates to P_8 to navigate the USV to avoid O_8 continuously [see Fig. 9(j)]. At T_{11}, the USV finds that there is no collision risk if it turns toward P_G, so the USV navigates to P_G directly until it reaches to P_G finally, as shown in Fig. 9(k) and Fig. 9(l).

C. EFFECT OF STEERING OCCASION

A virtual false dynamic obstacle O_d is set to simulate the influence of the steering occasion. If the algorithm does not adopt the steering occasion, then the USV alters its course immediately when it detects O_d. The trajectory acquired by this algorithm is shown in Fig. 10 and is composed of green and blue trajectory portions. In this case, the USV turns right to avoid a false obstacle when false information is detected. However, the USV finds that this information is false after several periods. Therefore, it turns left to navigate to the goal position again. Such redundant avoidance is not necessary. Instead, the USV will ignore the false obstacle at first if the steering occasion is adopted. The resulting trajectory is actually an optimal straight line, as shown by the dashed line in Fig. 10. By adopting a suitable steering occasion, the influence of false obstacles or large detection deviations of obstacles can be reduced.

D. COLLISION AVOIDANCE CONSIDERING COLREGs

In the algorithm, COLREGs restrict the feasible angle interval when the USV is going to avoid a collision with a moving vessel O_d. Fig. 11 to Fig. 13 show collision avoidance simulations considering COLREGs in three typical encounter situations. A USV-behind-overtaking situation is shown in Fig. 11, where COLREGs require the USV to give way to the overtaken vessel. As shown in Fig. 11(a), the USV detects O_d at time T_1. When the steering occasion is satisfied, the USV turns right to give way [see Fig. 11(b)]. When the USV overtakes O_d, it turns and sails to the goal position, as shown in Fig. 11(c). Figure 12 shows a head-on situation, and both the USV and O_d should alter their courses to starboard based on COLREGs. In this case, O_d is simulated to maintain its course, and the USV can still avoid it by turning right. It will be safer when O_d also alters its course under COLREGs. In the right-crossing situation, as shown in Fig. 13, the USV turns right and sails behind O_d to stay out of the way. All of these cases show the ability of the proposed algorithm to avoid a moving vessel based on COLREGs.

E. COLLISION AVOIDANCE IN ENVIRONMENT WITH STATIC AND DYNAMIC OBSTACLES

A simulation case in an environment with both static and dynamic obstacles is shown in Fig. 14. The USV trajectory moves from (0 m, 0 m) to (1900 m, 1900 m). Similar to the trajectory in Fig. 8, it consists of green and blue portions, and it considers COLREGs. Encounter situations with O_{d1} and O_{d3} are framed by rectangles. In the encounter situation with O_{d2}, the USV ignores O_{d2} because there is no collision risk between them. The detailed collision avoidance

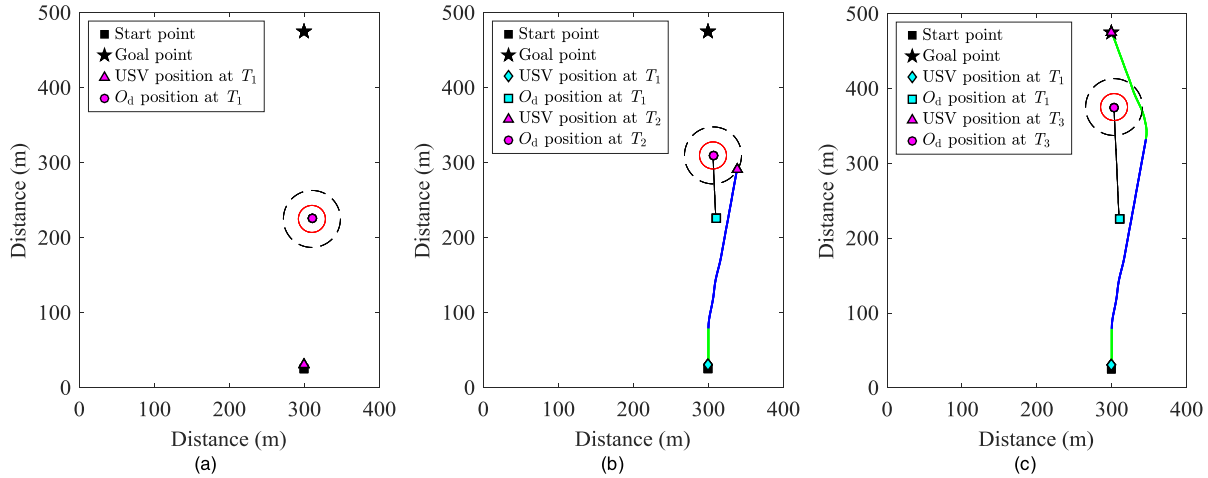

FIGURE 11. Collision avoidance process in USV-behind-overtaking situation, USV needs to give way to overtaken vessel O_d. (a) USV detects O_d at time T_1. (b) USV avoids collision by turning right when steering occasion is satisfied and overtakes O_d from starboard side of O_d. (c) USV overtakes O_d and sails toward goal point at T_3 which is last moment that USV detects O_d.

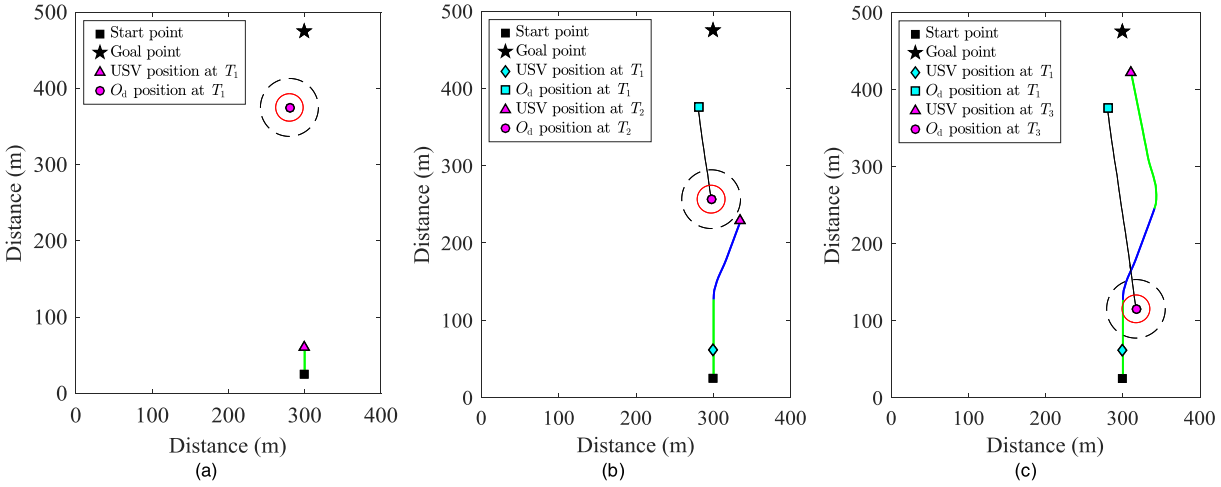

FIGURE 12. Collision avoidance process in head-on situation. In this case, moving vessel O_d keeps its speed and course, and should also give way based on COLREGs. Avoidance processes in (a), (b), and (c) are similar to those in Fig. 11.

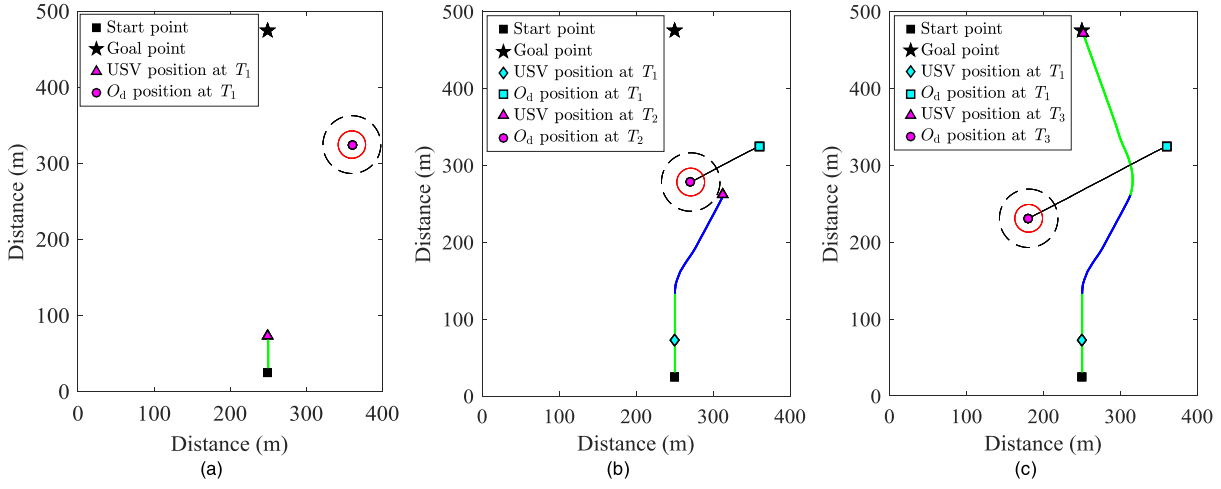

FIGURE 13. Collision avoidance process in right-crossing situation. USV needs to give way and sails behind moving vessel O_d to avoid collision. Avoidance processes in (a), (b), and (c) are similar to those in Fig. 11.

information of encounter situations with O_{d1} and O_{d3} are shown in Fig. 15 and Fig. 16 respectively. Both of these situations are crossing situations. The difference between them is that the USV takes the same avoidance maneuver in the encounter situation with O_{d1} regardless of whether the algorithm considers COLREGs; however, different avoidance

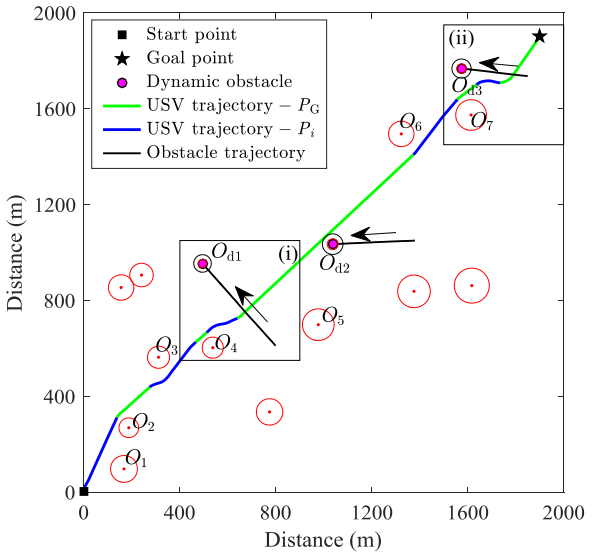

FIGURE 14. Collision avoidance considering COLREGs in an environment with both static and dynamic obstacles. Obstacle trajectories start when dynamic obstacles are detected and end when dynamic obstacles leave the detection range of the USV.

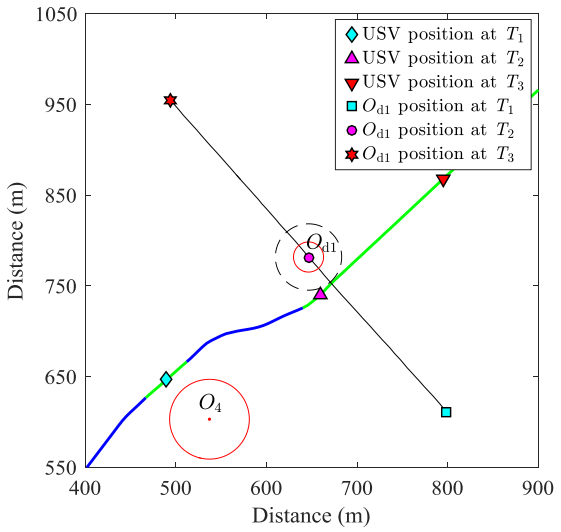

FIGURE 15. Collision avoidance processes in right-crossing situations between USV and dynamic obstacles O_{d1}. USV detects O_{d1} at T_1 for first time. It turns right to avoid collision and sails behind O_{d1}. O_{d1} is detected at T_3 for last time. In this situation, USV takes same avoidance maneuver by turning right whether algorithm considers COLREGs or not.

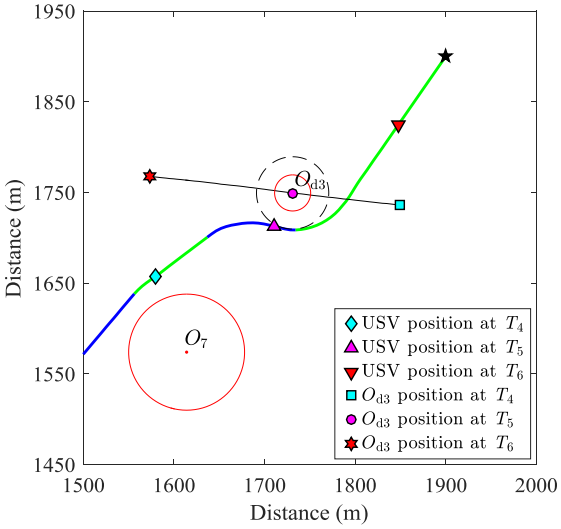

FIGURE 16. Collision avoidance processes in right-crossing situations between USV and dynamic obstacles O_{d3}. Avoidance process is similar to the that in Fig. 15 when algorithm considers COLREGs. However, USV turns left and sails in front of O_{d3}, as shown in Fig. 17.

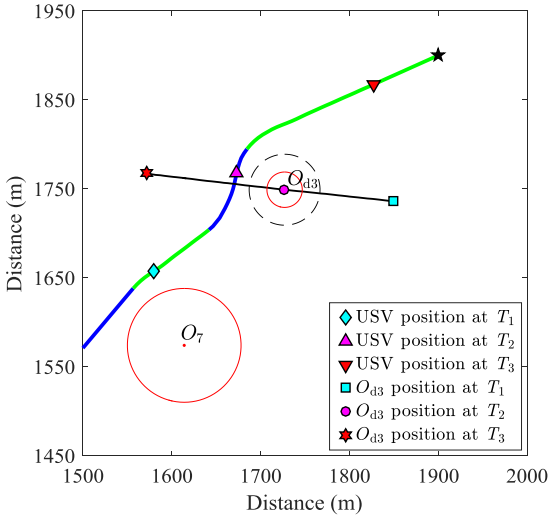

FIGURE 17. Collision avoidance process in right-crossing situation between the USV and O_{d3}. USV trajectory is acquired by algorithm, which does not consider COLREGs. In this situation, USV detects O_{d3} at T_4 and turns left to avoid collision when steering occasion is satisfied. This maneuver does not comply with Rule 15 of COLREGs.

maneuvers are taken in the encounter situation with O_{d3} when COLREGs are considered.

Fig. 15 shows the collision avoidance process in the encounter situation with O_{d1}. The USV detects O_{d1} at time T_1 for the first time and does not steer immediately. Then, the steering occasion is satisfied and the USV turns right to avoid collision. The positions and trajectories of the USV and O_{d1} at T_2 show that the USV sails safely behind O_{d1}. T_3 is the time at which O_{d1} is detected for the last time. The collision avoidance process in the encounter situation with O_{d3} is similar and is shown in Fig. 16. If the algorithm does not consider COLREGs, then the USV turns left and sails from the front of O_{d3}. The corresponding collision avoidance is shown in Fig. 17. This is not recommended based on Rule 15 of COLREGs.

VI. CONCLUSION AND FUTURE WORKS

A local collision avoidance algorithm based on steering maneuvers considering COLREGs was proposed for a USV

in environments with obstacles that are unknown before a mission. Under the dynamic constraints of the ''Jiuhang490'' USV, simulations in an environment with static obstacles alone or both static and dynamic obstacles were carried out. The results indicated the feasibility and validity of the algorithm.

This algorithm takes the steering maneuver alone at a constant speed to avoid collision for a USV in general situations. Such a maneuver is also suggested by COLREGs. In addition, the algorithm contains an emergency state in which collision avoidance cannot be achieved by a steering maneuver alone. In this situation, the algorithm can avoid collision by using other methods that alter the speed and heading of a USV simultaneously, such as the VO method. This process can ensure the functional integrity of the algorithm. In situations where the USV is a stand-on vessel, the steering occasion design can ensure that the USV will perform the necessary collision avoidance action when the other give-way vessel cannot perform effective collision avoidance. In addition, in the USV steering operation, the adopted a waypoint navigation method that seamlessly combines local collision avoidance with the global path. This is suitable for actual USVs using waypoint navigation technology, which is maturely applied.

In future work, an implementation of the proposed algorithm on the practical USV platform will be carried out to verify the actual performance. A combination with global path planning, such as the fast marching method, may be more effective in avoiding collisions in practical environments. Deep learning will be considered for research on large enough actions; this is required in Rule 8 of COLREGs. A virtual obstacle model that can respond to the USV motion is being constructed to study the effectiveness and feasibility of the algorithm when obstacles significantly alter their velocities.

REFERENCES

[1] S. Campbell, W. Naeem, and G. W. Irwin, ''A review on improving the autonomy of unmanned surface vehicles through intelligent collision avoidance manoeuvres,'' *Annu. Rev. Control*, vol. 36, no. 2, pp. 267–283, Dec. 2012.

[2] Z. Liu, Y. Zhang, X. Yu, and C. Yuan, ''Unmanned surface vehicles: An overview of developments and challenges,'' *Annu. Rev. Control*, vol. 41, pp. 71–93, Apr. 2016.

[3] M. Kurowski, A. Haghani, P. Koschorrek, and T. Jeinsch, ''Guidance, navigation and control of unmanned surface vehicles,'' *Automatisierungstechnik*, vol. 63, no. 5, pp. 355–367, Jan. 2015.

[4] P. Svec, M. Schwartz, A. Thakur, and S. K. Gupta, ''Trajectory planning with look-ahead for unmanned sea surface vehicles to handle environmental disturbances,'' in *Proc. IROS*, San Francisco, CA, USA, Sep. 2011, pp. 1154–1159.

[5] R. A. Soltan, H. Ashrafiuon, and K. R. Muske, ''Trajectory real-time obstacle avoidance for underactuated unmanned surface vessels,'' in *Proc. IDETC/CIE*, San Diego, CA, USA, Jan. 2009, pp. 1059–1067.

[6] Z. Du, Y. Wen, C. Xiao, F. Zhang, L. Huang, and C. Zhou, ''Motion planning for unmanned surface vehicle based on trajectory unit,'' *Ocean Eng.*, vol. 151, pp. 46–56, Mar. 2018.

[7] Y. Wang, X. Yu, X. Liang, and B. Li, ''A COLREGs-based obstacle avoidance approach for unmanned surface vehicles,'' *Ocean Eng.*, vol. 169, pp. 110–124, Dec. 2018.

[8] P. Fiorini and Z. Shiller, ''Motion planning in dynamic environments using velocity obstacles,'' *Int. J. Robot. Res.*, vol. 17, no. 7, pp. 760–772, Jul. 1998.

[9] Y. Kuwata, M. T. Wolf, D. Zarzhitsky, and T. L. Huntsberger, ''Safe maritime autonomous navigation with COLREGS, using velocity obstacles,'' *IEEE J. Ocean. Eng.*, vol. 39, no. 1, pp. 110–119, Jan. 2014.

[10] Y. Huang, P. H. A. J. M. van Gelder, and Y. Wen, ''Velocity obstacle algorithms for collision prevention at sea,'' *Ocean Eng.*, vol. 151, pp. 308–321, Mar. 2018.

[11] Y. Huang, L. Chen, and P. H. A. J. M. van Gelder, ''Generalized velocity obstacle algorithm for preventing ship collisions at sea,'' *Ocean Eng.*, vol. 173, pp. 142–156, Feb. 2019.

[12] Y. Cho, J. Han, J. Kim, P. Lee, and S.-B. Park, ''Experimental validation of a velocity obstacle based collision avoidance algorithm for unmanned surface vehicles,'' *IFAC-PapersOnLine*, vol. 52, no. 21, pp. 329–334, Dec. 2019.

[13] R. Zhang, P. Tang, Y. Su, X. Li, G. Yang, and C. Shi, ''An adaptive obstacle avoidance algorithm for unmanned surface vehicle in complicated marine environments,'' *IEEE/CAA J. Autom. Sinica*, vol. 1, no. 4, pp. 385–396, Oct. 2014.

[14] P. Tang, R. Zhang, D. Liu, L. Huang, G. Liu, and T. Deng, ''Local reactive obstacle avoidance approach for high-speed unmanned surface vehicle,'' *Ocean Eng.*, vol. 106, pp. 128–140, Sep. 2015.

[15] T. Praczyk, ''Neural anti-collision system for autonomous surface vehicle,'' *Neurocomputing*, vol. 149, pp. 559–572, Feb. 2015.

[16] L. Zhao and M.-I. Roh, ''COLREGs-compliant multiship collision avoidance based on deep reinforcement learning,'' *Ocean Eng.*, vol. 191, pp. 1–15, Oct. 2019.

[17] H. Shen, H. Hashimoto, A. Matsuda, Y. Taniguchi, D. Terada, and C. Guo, ''Automatic collision avoidance of multiple ships based on deep *Q*-learning,'' *Appl. Ocean Res.*, vol. 86, pp. 268–288, May 2019.

[18] *International Regulations for Prevention of Collisions at Sea, 1972 (72 COLREGS)*, US Dept. Transp., US Coast Guard, UCG, Commandant Instruct., Washington, DC, USA, 1999.

[19] M. R. Benjamin, J. J. Leonard, J. A. Curcio, and P. M. Newman, ''A method for protocol-based collision avoidance between autonomous marine surface craft,'' *J. Field Robot.*, vol. 23, no. 5, pp. 333–346, May 2006.

[20] M. Candeloro, A. M. Lekkas, and A. J. Sørensen, ''A Voronoi-diagram-based dynamic path-planning system for underactuated marine vessels,'' *Control Eng. Pract.*, vol. 61, pp. 41–54, Apr. 2017.

[21] R. M. Keller, *Computer Science: Abstraction to Implementation*. Claremont, CA, USA: Harvey Mudd College, 2001.

[22] H. C. Woithe and U. Kremer, ''A programming architecture for smart autonomous underwater vehicles,'' in *Proc. IROS*, St. Louis, MO, USA, Oct. 2009, pp. 4433–4438.

[23] H. L. Xu and X. S. Feng, ''An AUV fuzzy obstacle avoidance method under event feedback supervision,'' in *Proc. OCEANS*, Biloxi, MS, USA, Oct. 2009, pp. 1–6.

[24] S. B. Saad, B. Zerr, I. Probst, and F. Dambreville, ''Hybrid coordination strategy of a group of cooperating autonomous underwater vehicles,'' *IFAC-PapersOnLine*, vol. 48, no. 5, pp. 47–52, Jun. 2015.

[25] J. Redding, J. Amin, J. Boskovic, and J. Jackson, ''Collaborative mission planning, autonomy and control technology (CoMPACT) for unmanned surface vehicles,'' in *Proc. AIAA*, Chicago, IL, USA, Aug. 2009, p. 5774.

[26] L. Elkins, D. Sellers, and W. R. Monach, ''The autonomous maritime navigation (AMN) project: Field tests, autonomous and cooperative behaviors, data fusion, sensors, and vehicles,'' *J. Field Robot.*, vol. 27, no. 6, pp. 790–818, Nov. 2010.

[27] D. Wang, J. Zhang, J. Jin, F. Shao, and X. Mao, ''A steering occasion strategy for local collision avoidance of an unmanned surface vehicle in a complex environment,'' in *Proc. CCC*, Dalian, China, Jul. 2017, pp. 6133–6138.

[28] Y. He, Y. Jin, L. Huang, Y. Xiong, P. Chen, and J. Mou, ''Quantitative analysis of COLREG rules and seamanship for autonomous collision avoidance at open sea,'' *Ocean Eng.*, vol. 140, pp. 281–291, Aug. 2017.

[29] Y. Zhao, W. Li, and P. Shi, ''A real-time collision avoidance learning system for unmanned surface vessels,'' *Neurocomputing*, vol. 182, pp. 255–266, Mar. 2016.

[30] C. Tam and R. Bucknall, ''Cooperative path planning algorithm for marine surface vessels,'' *Ocean Eng.*, vol. 57, pp. 25–33, Jan. 2013.

[31] J. Jin, J. Zhang, D. Liu, F. Shao, D. Wang, J. Shi, and F. Li, ''Design and experiment for an offshore nuclear radiation emergent observation system based on an unmanned surface vehicle,'' *J. Coastal Res.*, vol. 90, pp. 35–40, Mar. 2019.

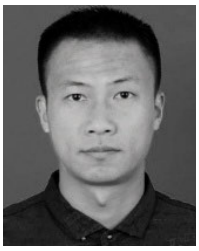

DONG WANG received the B.S. degree from Zhejiang University, China, in 2010, and the M.S. degree from the Ocean University of China, China, in 2013. He is currently pursuing the Ph.D. degree with the Harbin Institute of Technology, China. His research interests include path planning, collision avoidance, and autonomous control of unmanned surface vehicles.

JIE ZHANG received the B.S. and M.S. degrees from Inner Mongolia University, China, in 1984 and 1987, respectively, and the Ph.D. degree from Tsinghua University, China. He then stayed at Inner Mongolia University as a Lecturer until 1990. He is currently a Researcher with the First Institute of Oceanography, Ministry of Natural Resources, and the Leader of the College of Oceanography and Space Informatics, China University of Petroleum. His research interests include surveillance technology and equipment for maritime targets in exclusive economic zone, research and development of autonomous satellite remote sensing technology, and coastal high-resolution remote sensing technology and application.

JIUCAI JIN received the B.S. and M.S. degrees in physics from Inner Mongolia University, China, in 2001 and 2005, respectively, and the Ph.D. degree in physical oceanography from the Institute of Oceanology, Chinese Academy of Sciences, in 2011. He is currently an Associate Researcher with the First Institute of Oceanography, Ministry of Natural Resources. His research interests include modeling, autonomous control, obstacle avoidance, development for unmanned surface vehicle, and applications of USV.

XINGPENG MAO (Member, IEEE) received the B.S. degree in radio electronics from Northeast Normal University, China, in 1993, and the M.S. and Ph.D. degrees in communication and information system from the Harbin Institute of Technology, China, in 1999 and 2004, respectively. He is currently a Professor with HIT. His research interests include array signal processing, communication and radar system design, and the theory on advanced radar systems.